# The Fluid Mechanics of Airway Closure in the Bronchioles

Francesco Romanò
Department of Fluid Mechanics and Energetics, Arts et Métiers, Lille

*Thanks to:* J.B. Grotberg, M. Muradoglu, H. Fujioka, O. Erken

Dept. of Physics, University of Rome Tor Vergata, Rome, Italy
January 16, 2023

# Airway Closure in Physiology

## Morphology

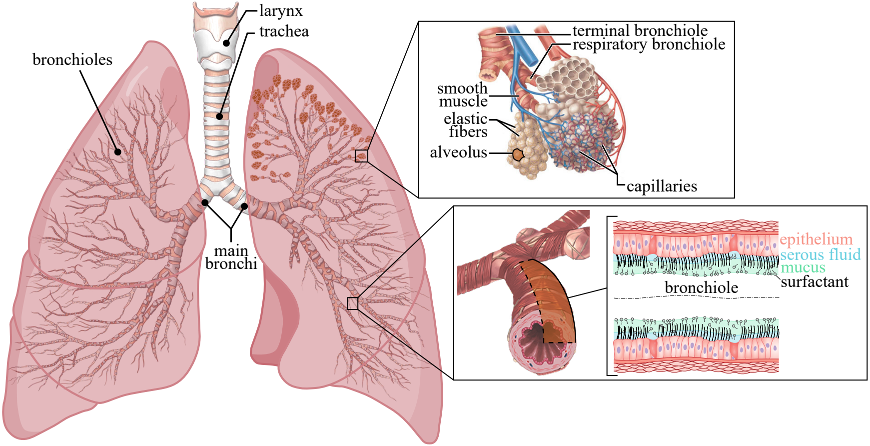

# Airway Closure in Physiology

## Morphology: $d_n = d_0 \times 2^{n/3}$

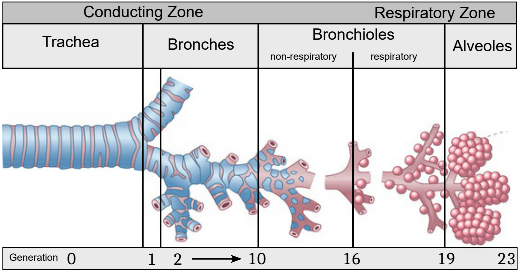


| Generation | Diameter (cm) | Length (cm) |
|---|---|---|
| 0 (Trachea) | 1.8 | 12 |
| 1 | 1.220 | 4.760 |
| 2 | 0.830 | 1.900 |
| 10 | 0.130 | 0.460 |
| 16 | 0.060 | 0.165 |
| 19 | 0.047 | 0.099 |
| 23 | 0.041 | 0.050 |

# Airway Closure in Physiology

## Morphology: $d_n = d_0 \times 2^{n/3}$

$$\boxed{Bo = \frac{ga^2(\rho_L - \rho_G)}{\sigma_0}}$$

$a$: airway radius
$\rho_L$: liquid layer density
$\rho_G$: gas core density
$g$: gravity acceleration
$\sigma_0$: liquid-gas surface tension

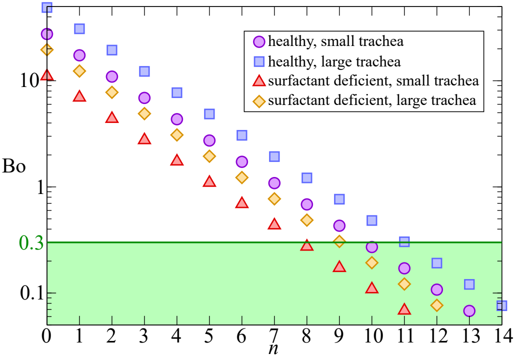


# Airway Closure in Physiology

## Morphology: $d_n = d_0 \times 2^{n/3}$

$$\boxed{Bo = \frac{ga^2(\rho_\mathrm{L} - \rho_\mathrm{G})}{\sigma_0}}$$

$a$: airway radius
$\rho_\mathrm{L}$: liquid layer density
$\rho_\mathrm{G}$: gas core density
$g$: gravity acceleration
$\sigma_0$: liquid-gas surface tension

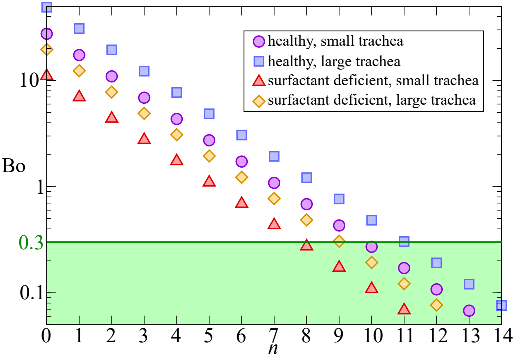


gravity negligible from ≈ 7th generation on

# Surface Tension

## Molecular Scale

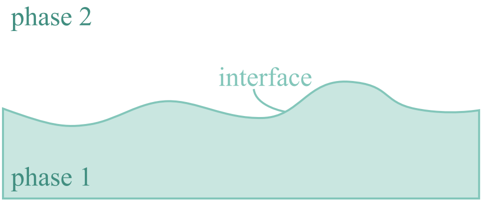

# Surface Tension

## Molecular Scale

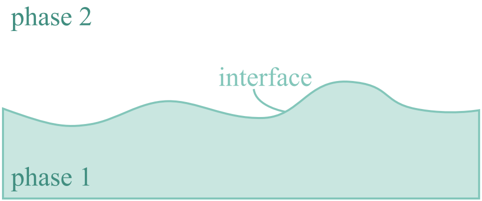


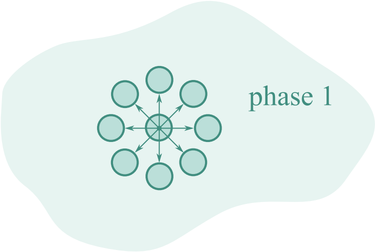

# Surface Tension

## Molecular Scale

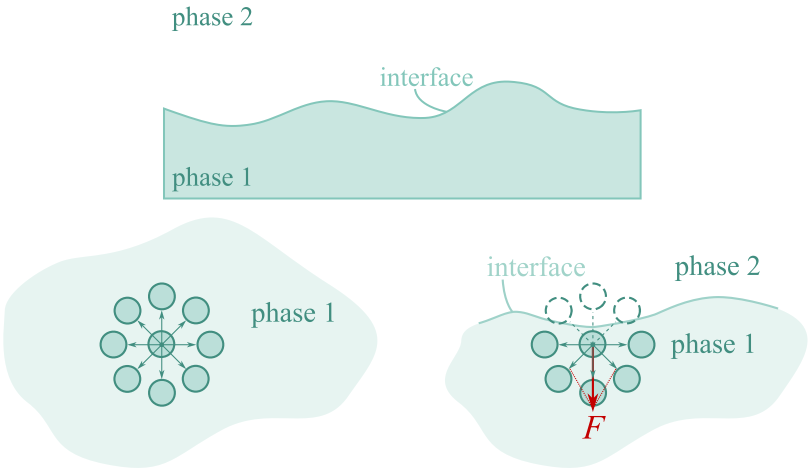

# Surface Tension

## Macroscopic Scale

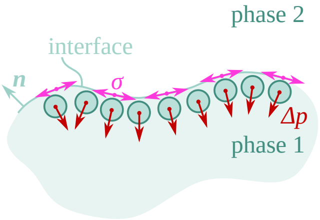

# Surface Tension

## Macroscopic Scale

Young–Laplace equation: $\Delta p = -\sigma \nabla \cdot \boldsymbol{n}$

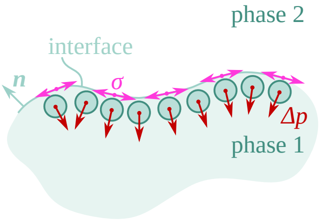

# Surface Tension

## Macroscopic Scale

Young–Laplace equation: $\Delta p = -\sigma \nabla \cdot \boldsymbol{n}$

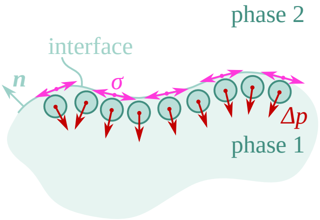


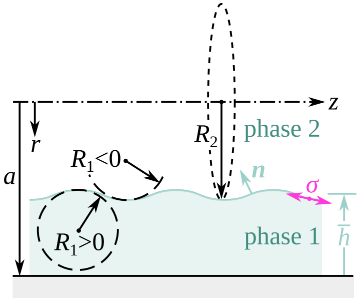

# Surface Tension

## Macroscopic Scale

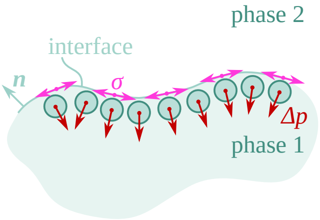


Young–Laplace equation: $\Delta p = -\sigma \nabla \cdot \boldsymbol{n}$

Curvature in cylindrical coordinates: $-\nabla \cdot \boldsymbol{n} = \left( \frac{1}{R_1} + \frac{1}{R_2} \right)$

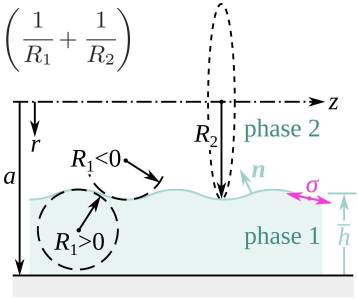

# Surface Tension

## Macroscopic Scale

Young–Laplace equation: $\Delta p = -\sigma \nabla \cdot \boldsymbol{n}$

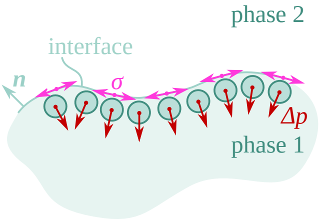


Curvature in cylindrical coordinates: $-\nabla \cdot \boldsymbol{n} = \left( \frac{1}{R_1} + \frac{1}{R_2} \right)$

$R_1 = -(d_z^2 h)^{-1}$

$R_2 = a - h$

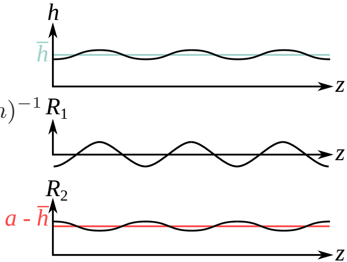


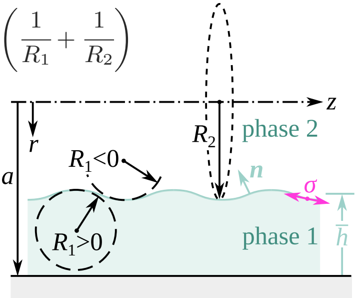

# Plateau–Rayleigh Instability

## Instability Mechanism

Assuming a varicose perturbation: $h = \bar{h}[1 + A\sin(kz)]$

# Plateau–Rayleigh Instability

## Instability Mechanism

Assuming a varicose perturbation: $h = \bar{h}[1 + A\sin(kz)]$

- Effect of in-plane curvature $R_1^{-1} \sim \left[\bar{h}Ak^2 \sin(kz)\right]$

# Plateau–Rayleigh Instability

## Instability Mechanism

Assuming a varicose perturbation: $h = \bar{h}[1 + A\sin(kz)]$

- Effect of in-plane curvature $R_1^{-1} \sim \left[\bar{h}Ak^2 \sin(kz)\right]$

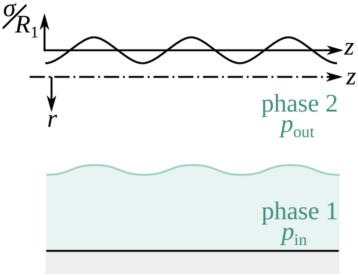

# Plateau–Rayleigh Instability

## Instability Mechanism

Assuming a varicose perturbation: $h = \bar{h}[1 + A\sin(kz)]$

- Effect of in-plane curvature $R_1^{-1} \sim \left[\bar{h}Ak^2\sin(kz)\right]$

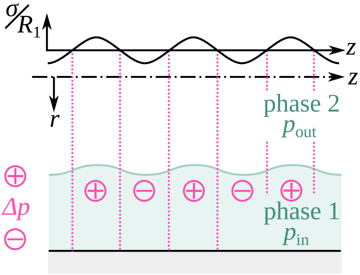

# Plateau–Rayleigh Instability

## Instability Mechanism

Assuming a varicose perturbation: $h = \bar{h}[1 + A\sin(kz)]$

- Effect of in-plane curvature $R_1^{-1} \sim \left[\bar{h}Ak^2 \sin(kz)\right]$

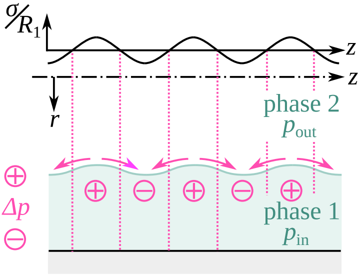

# Plateau–Rayleigh Instability

## Instability Mechanism

Assuming a varicose perturbation: $h = \bar{h}[1 + A\sin(kz)]$

- Effect of in-plane curvature $R_1^{-1} \sim \left[\bar{h}Ak^2 \sin(kz)\right]$

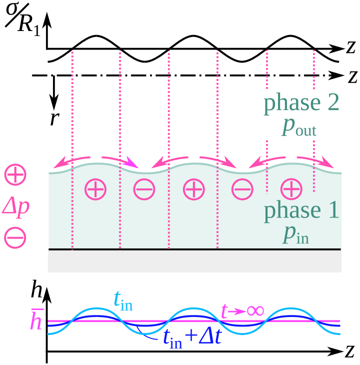

# Plateau–Rayleigh Instability

## Instability Mechanism

Assuming a varicose perturbation: $h = \bar{h}[1 + A\sin(kz)]$

- Effect of in-plane curvature $R_1^{-1} \sim \left[\bar{h}Ak^2 \sin(kz)\right]$

  $\rightarrow$ The in-plane curvature has a stabilizing effect with $R_1 \ \sim k^2$

# Plateau–Rayleigh Instability

## Instability Mechanism

Assuming a varicose perturbation: $h = \bar{h}[1 + A\sin(kz)]$

- ▷ Effect of in-plane curvature $R_1^{-1} \sim \left[\bar{h}Ak^2\sin(kz)\right]$

  $\rightarrow$ The in-plane curvature has a stabilizing effect with $R_1 \sim k^2$

- ▷ Effect of cross-sectional curvature $R_2^{-1} \sim \left\{a - \bar{h}[1 + A\sin(kz)]\right\}^{-1}$

# Plateau–Rayleigh Instability

## Instability Mechanism

Assuming a varicose perturbation: $h = \bar{h}[1 + A\sin(kz)]$

- ▷ Effect of in-plane curvature $R_1^{-1} \sim \left[\bar{h}Ak^2\sin(kz)\right]$

  → The in-plane curvature has a stabilizing effect with $R_1 \ \sim k^2$

- ▷ Effect of cross-sectional curvature $R_2^{-1} \sim \left\{a - \bar{h}[1 + A\sin(kz)]\right\}^{-1}$

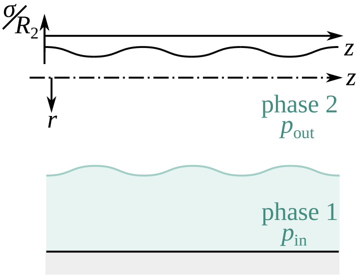

# Plateau–Rayleigh Instability

## Instability Mechanism

Assuming a varicose perturbation: $h = \bar{h}[1 + A\sin(kz)]$

- ▷ Effect of in-plane curvature $R_1^{-1} \sim \left[\bar{h}Ak^2 \sin(kz)\right]$

  $\rightarrow$ The in-plane curvature has a stabilizing effect with $R_1 \ \sim k^2$

- ▷ Effect of cross-sectional curvature $R_2^{-1} \sim \left\{a - \bar{h}[1 + A\sin(kz)]\right\}^{-1}$

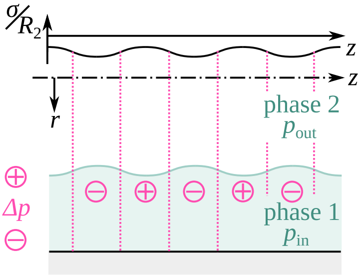

# Plateau–Rayleigh Instability

## Instability Mechanism

Assuming a varicose perturbation: $h = \bar{h}[1 + A\sin(kz)]$

- ▷ Effect of in-plane curvature $R_1^{-1} \sim \left[\bar{h}Ak^2 \sin(kz)\right]$

  $\rightarrow$ The in-plane curvature has a stabilizing effect with $R_1 \sim k^2$

- ▷ Effect of cross-sectional curvature $R_2^{-1} \sim \left\{a - \bar{h}[1 + A\sin(kz)]\right\}^{-1}$

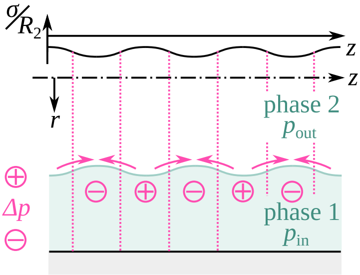

# Plateau–Rayleigh Instability

## Instability Mechanism

Assuming a varicose perturbation: $h = \bar{h}[1 + A\sin(kz)]$

- Effect of in-plane curvature $R_1^{-1} \sim \left[\bar{h}Ak^2 \sin(kz)\right]$

  $\rightarrow$ The in-plane curvature has a stabilizing effect with $R_1 \sim k^2$

- Effect of cross-sectional curvature $R_2^{-1} \sim \left\{a - \bar{h}[1 + A\sin(kz)]\right\}^{-1}$

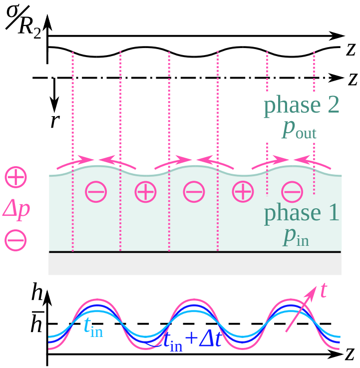

# Plateau–Rayleigh Instability

## Instability Mechanism

Assuming a varicose perturbation: $h = \bar{h}[1 + A\sin(kz)]$

- ▷ Effect of in-plane curvature $R_1^{-1} \sim \left[\bar{h}Ak^2 \sin(kz)\right]$

  $\rightarrow$ The in-plane curvature has a stabilizing effect with $R_1 \sim k^2$

- ▷ Effect of cross-sectional curvature $R_2^{-1} \sim \left\{a - \bar{h}[1 + A\sin(kz)]\right\}^{-1}$

  $\rightarrow$ The cross-sectional curvature has a destabilizing effect with $R_2 \sim a - \bar{h}$

# Plateau–Rayleigh Instability

## Instability Mechanism

Assuming a varicose perturbation: $h = \bar{h}[1 + A\sin(kz)]$

- ▷ Effect of in-plane curvature $R_1^{-1} \sim \left[\bar{h}Ak^2 \sin(kz)\right]$

  $\rightarrow$ The in-plane curvature has a stabilizing effect with $R_1 \sim k^2$

- ▷ Effect of cross-sectional curvature $R_2^{-1} \sim \left\{a - \bar{h}[1 + A\sin(kz)]\right\}^{-1}$

  $\rightarrow$ The cross-sectional curvature has a destabilizing effect with $R_2 \sim a - \bar{h}$

For a given $\bar{h}/a$ one can find the critical wavenumber $k_c$

# Airway Closure in Physiology

## Breathing Cycle

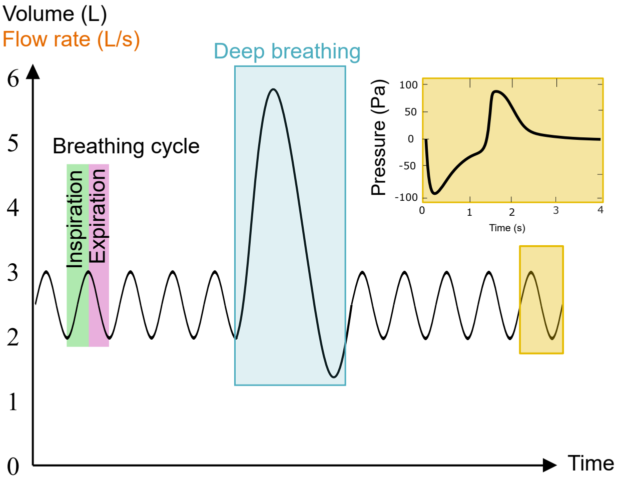

# Airway Closure in Physiology

## Breathing Cycle

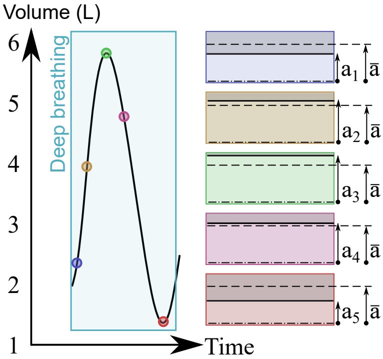

# Airway Closure in Physiology

## Breathing Cycle

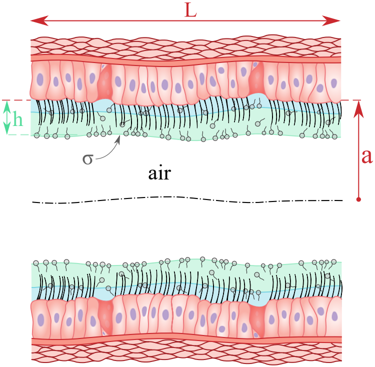


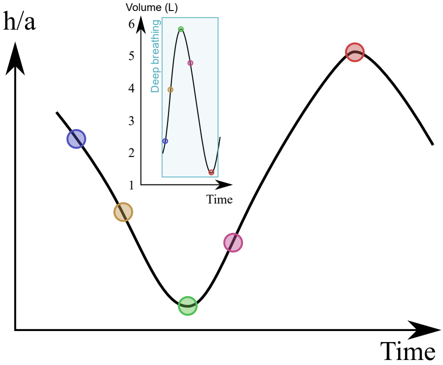


# Airway Closure in Physiology

## Breathing Cycle

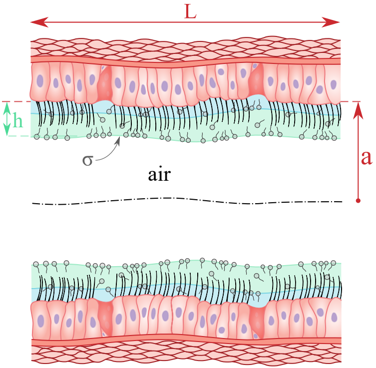


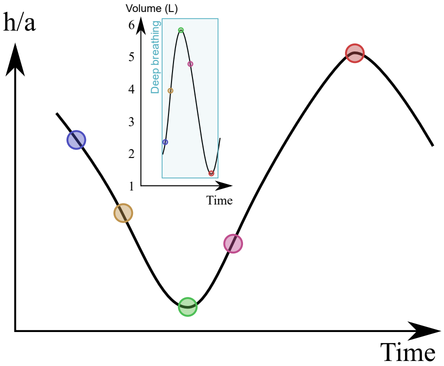


Young–Laplace equation: $\Delta p = -\sigma \nabla \cdot \boldsymbol{n}$

Plateau–Rayleigh instability: $2\pi(a - h)/L < 0.698$

# Airway Closure in Physiology

## Breathing Cycle

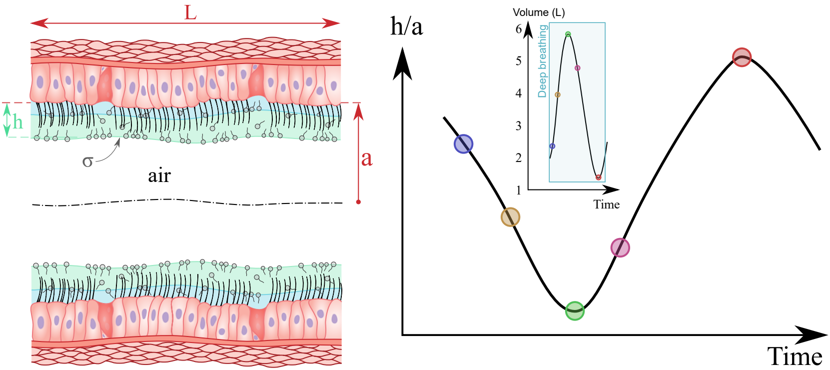


Young–Laplace equation: $\Delta p = -\sigma \nabla \cdot \boldsymbol{n}$

Plateau–Rayleigh instability: $2\pi(a-h)/L < 0.698$

Plateau–Rayleigh instability during deep exhalation in distal airways

# Airway Closure in Physiology

## Impact on the Epithelium

Huh et al.
PNAS (2007)

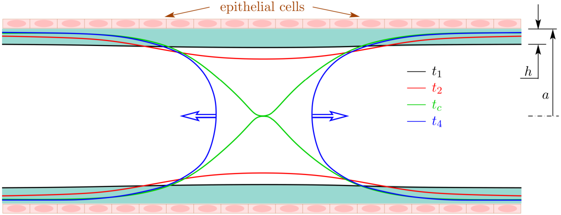


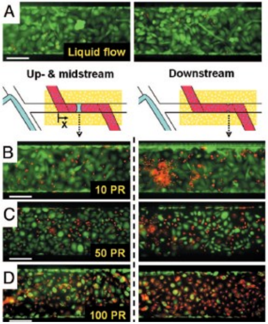

# Airway Closure in Physiology

## Impact on the Epithelium

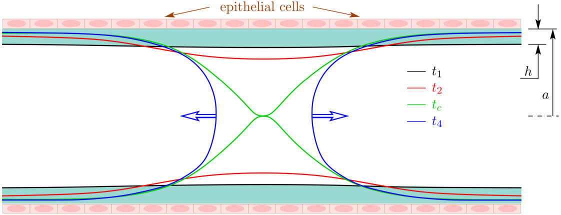


Huh et al.
PNAS (2007)

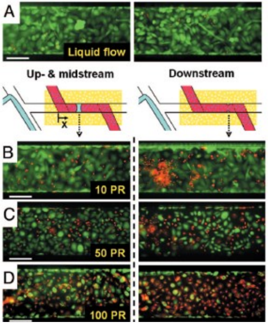


airway closure may induce lethal or sub-lethal responses for epithelial cells

# Modeling Challenges

## Physiological Airways

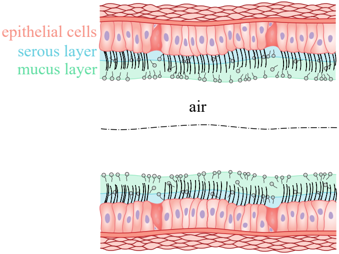


- complex multilayer structure
- ciliated surface
- fluid structure interaction
- complex multiphase flow
- non-Newtonian two-layer liquid
- surfactant dynamics

# Modeling Challenges

## Physiological Airways

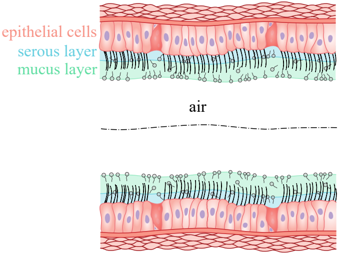


- complex multilayer structure
- ciliated surface
- fluid structure interaction
- complex multiphase flow
- non-Newtonian two-layer liquid
- surfactant dynamics

## Airways Modeling

- rigid airway walls
- no through flow
- periodic conditions
- complex multiphase flow
- non-Newtonian two-layer
- surfactant dynamics

# Modeling Challenges

## Physiological Airways

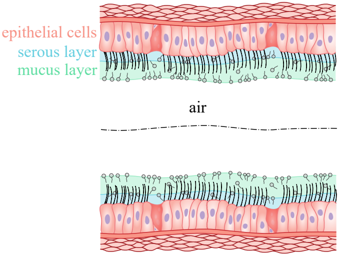


- complex multilayer structure
- ciliated surface
- fluid structure interaction
- complex multiphase flow
- non-Newtonian two-layer liquid
- surfactant dynamics

## Airways Modeling

- rigid airway walls
- no through flow
- periodic conditions
- complex multiphase flow
- non-Newtonian two-layer
- surfactant dynamics

## Scientific Approach

- Newtonian single-layer clean

# Modeling Challenges

## Physiological Airways

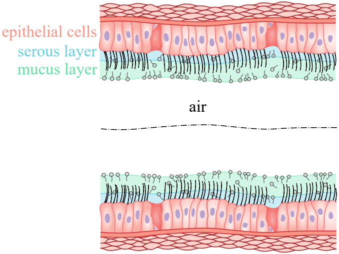


- complex multilayer structure
- ciliated surface
- fluid structure interaction
- complex multiphase flow
- non-Newtonian two-layer liquid
- surfactant dynamics

## Airways Modeling

- rigid airway walls
- no through flow
- periodic conditions
- complex multiphase flow
- non-Newtonian two-layer
- surfactant dynamics

## Scientific Approach

- Newtonian single-layer clean
- Newtonian two-layer clean

# Modeling Challenges

## Physiological Airways

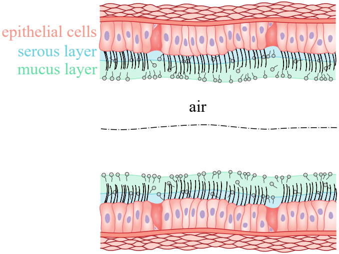


- complex multilayer structure
- ciliated surface
- fluid structure interaction
- complex multiphase flow
- non-Newtonian two-layer liquid
- surfactant dynamics

## Airways Modeling

- rigid airway walls
- no through flow
- periodic conditions
- complex multiphase flow
- non-Newtonian two-layer
- surfactant dynamics

## Scientific Approach

- Newtonian single-layer clean
- Newtonian two-layer clean
- viscoelastic single-layer clean

# Modeling Challenges

## Physiological Airways

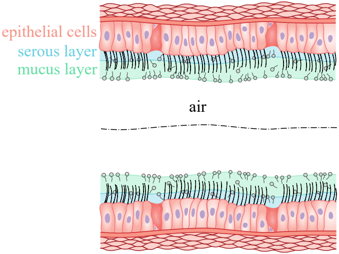


- complex multilayer structure
- ciliated surface
- fluid structure interaction
- complex multiphase flow
- non-Newtonian two-layer liquid
- surfactant dynamics

## Airways Modeling

- rigid airway walls
- no through flow
- periodic conditions
- complex multiphase flow
- non-Newtonian two-layer
- surfactant dynamics

## Scientific Approach

- Newtonian single-layer clean
- Newtonian two-layer clean
- viscoelastic single-layer clean
- Newtonian single-layer + surf.

# Newtonian Airway Closure

Romanò et al., PRF (2019)

## Mathematical Model

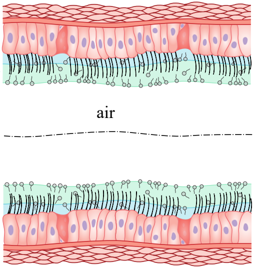


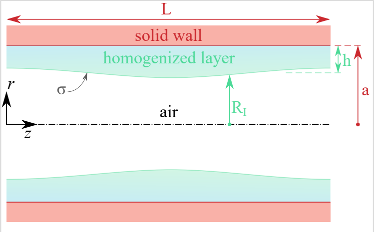


Newtonian airway closure model (clean)

$$\nabla \cdot \boldsymbol{u} = 0$$

$$\mathrm{La}\left[\frac{\partial\left(\tilde{\varrho}\boldsymbol{u}\right)}{\partial t} + \nabla\cdot\left(\tilde{\varrho}\boldsymbol{u}\boldsymbol{u}\right)\right] = -\nabla p + \nabla\cdot\left[\tilde{\mu}\left(\nabla\boldsymbol{u} + \nabla^T\boldsymbol{u}\right)\right] + \int_A \sigma\kappa\boldsymbol{n}\delta\left(\boldsymbol{x}-\boldsymbol{x}_{\mathrm{f}}\right) dA$$

# Newtonian Airway Closure

Romanò et al., PRF (2019)

## Mathematical Model

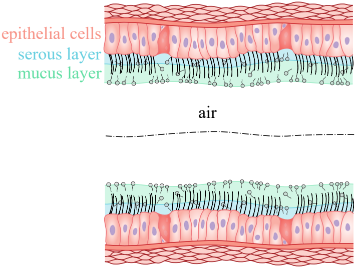


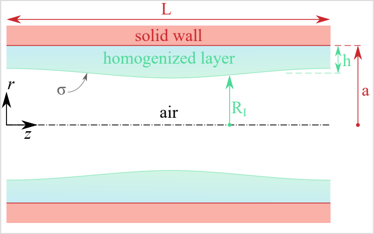


Newtonian airway closure model (clean)

$$\nabla \cdot \boldsymbol{u} = 0$$

$$\mathrm{La}\left[\frac{\partial\left(\tilde{\varrho}\boldsymbol{u}\right)}{\partial t} + \nabla\cdot\left(\tilde{\varrho}\boldsymbol{u}\boldsymbol{u}\right)\right] = -\nabla p + \nabla\cdot\left[\tilde{\mu}\left(\nabla\boldsymbol{u} + \nabla^T\boldsymbol{u}\right)\right] + \int_A \sigma\kappa\boldsymbol{n}\delta\left(\boldsymbol{x} - \boldsymbol{x}_\mathrm{f}\right)dA$$

Single-field approach: $\tilde{\varrho} = \phi + \varrho(1-\phi), \quad \tilde{\mu} = \phi + \mu(1-\phi)$

Non-dimensional groups: $\mathrm{La} = \dfrac{\sigma\rho_\mathrm{L} a}{\mu_\mathrm{L}^2},\ \varrho = \dfrac{\rho_\mathrm{G}}{\rho_\mathrm{L}},\ \mu = \dfrac{\mu_\mathrm{G}}{\mu_\mathrm{L}},\ \lambda = \dfrac{L}{a},\ \varepsilon = \dfrac{h}{a}$

Initial perturbation: $r = R_\mathrm{I}(t=0) = a - h[1 - 0.1\times\cos(2\pi z/L)]$

# Newtonian Airway Closure

Romanò et al., PRF (2019)

## Comparison with Experiments

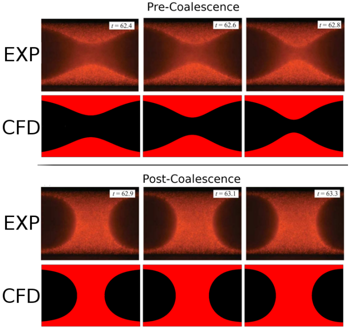


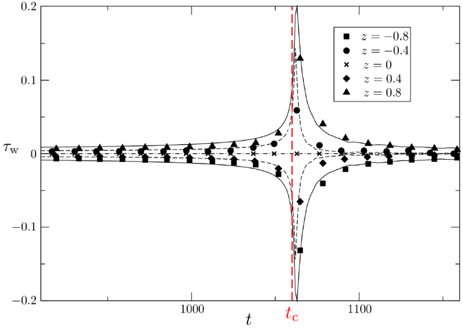


Exp: Bian et al., JFM (2010)
CFD: Romanò et al., PRF (2019)

Markers: Bian et al., JFM (2010)
Lines: Romanò et al., PRF (2019)

# Newtonian Airway Closure

Romanò et al., PRF (2019)

## Comparison with Experiments

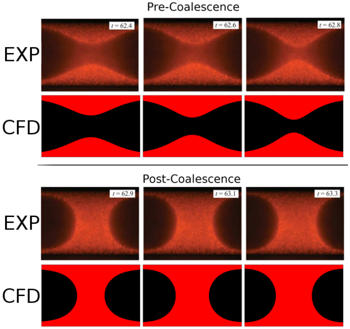


Exp: Bian et al., JFM (2010)
CFD: Romanò et al., PRF (2019)

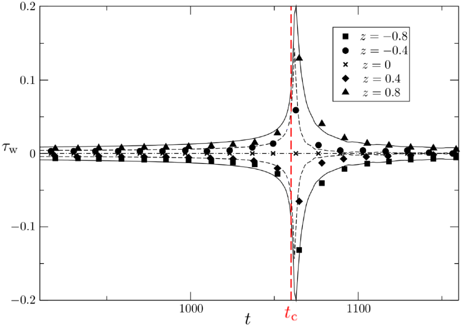


Markers: Bian et al., JFM (2010)
Lines: Romanò et al., PRF (2019)

peak of shear stress right after closure ($t_c$)

# Newtonian Airway Closure

Romanò et al., PRF (2019)

## Bi-frontal Plug Growth

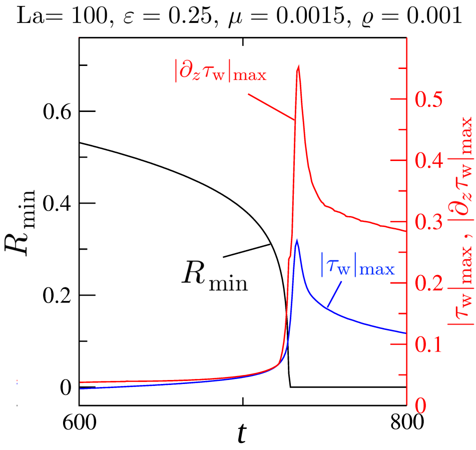


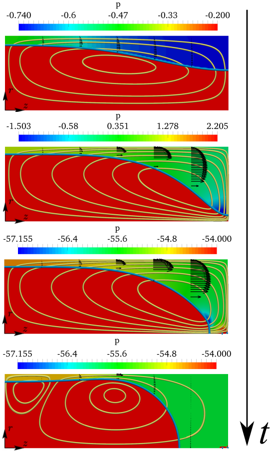

# Newtonian Airway Closure

Romanò et al., PRF (2019)

## Bi-frontal Plug Growth

La$= 100$, $\varepsilon = 0.25$, $\mu = 0.0015$, $\varrho = 0.001$

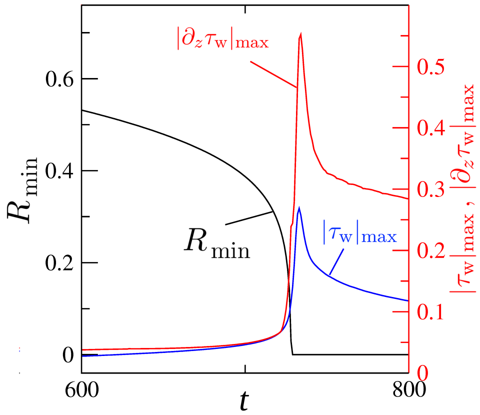


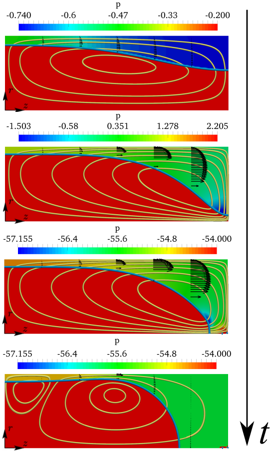


Plateau–Rayleigh instability and rapid bi-frontal plug growth

# Newtonian Airway Closure

Romanò et al., PRF (2019)

## Bi-frontal Plug Growth

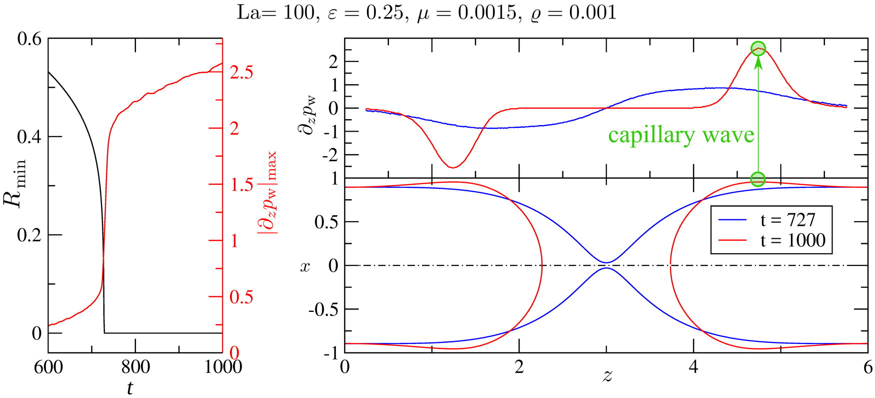

# Newtonian Airway Closure

Romanò et al., PRF (2019)

## Bi-frontal Plug Growth

La= 100, $\varepsilon = 0.25$, $\mu = 0.0015$, $\varrho = 0.001$

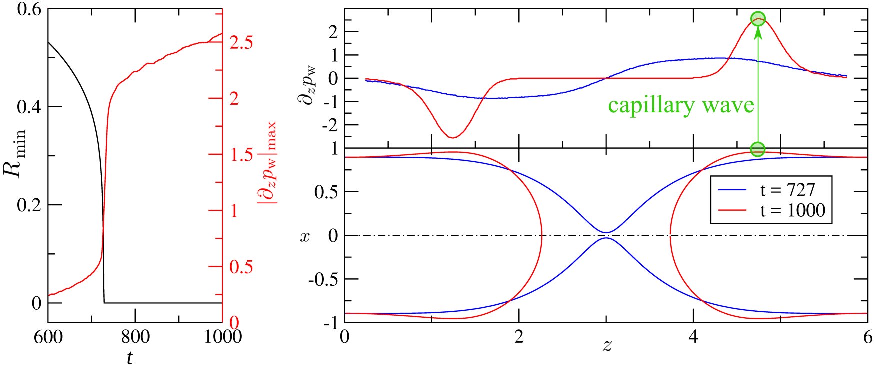


bi-frontal plug growth correlated to the wall pressure gradient

# Newtonian Airway Closure

Romanò et al., PRF (2019)

## Bi-frontal Plug Growth

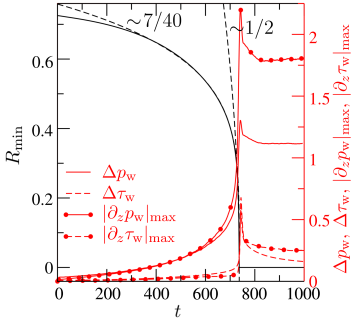


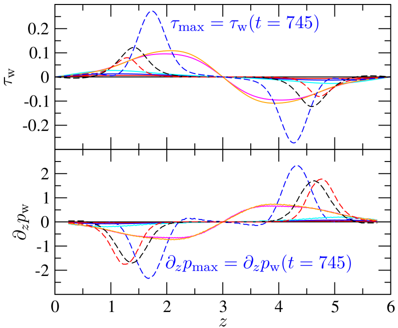


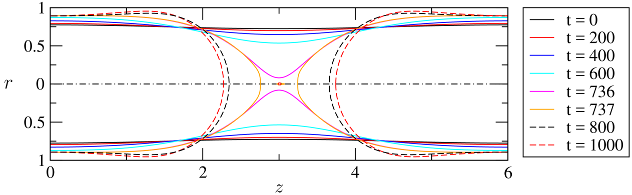

# Newtonian Airway Closure

Romanò et al., PRF (2019)

## Effect of Film Thickness

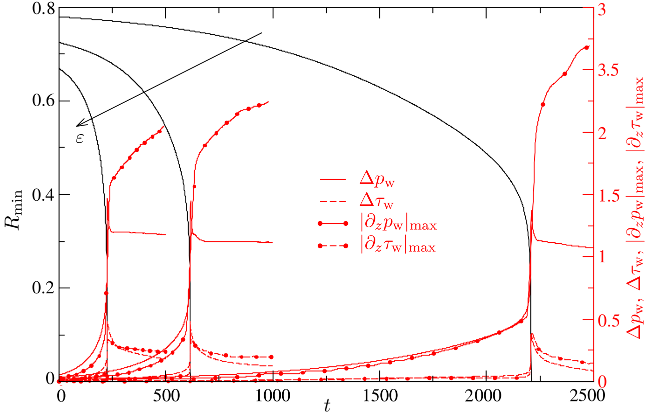

# Newtonian Airway Closure

Romanò et al., PRF (2019)

## Effect of Film Thickness

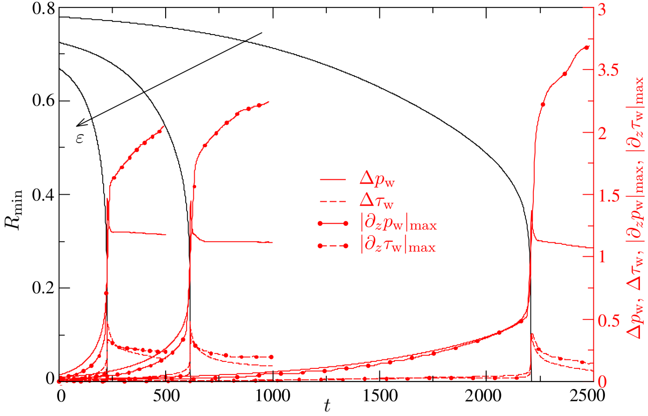


increasing $\varepsilon$ speeds up the closure and reduces the wall pressure gradient

# Newt. Two-Layer Airway Closure

Erken et al., JFM (2022)

## Mathematical Model

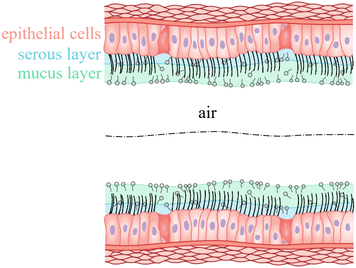


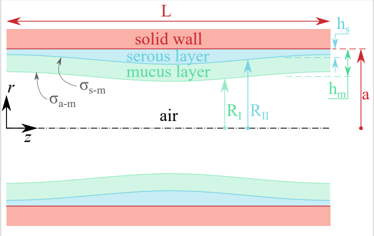


Newtonian two-layer airway closure model (clean)

$$\nabla \cdot \boldsymbol{u} = 0$$

$$\mathrm{La}\left[\frac{\partial\left(\tilde{\varrho}\boldsymbol{u}\right)}{\partial t} + \nabla\cdot\left(\tilde{\varrho}\boldsymbol{u}\boldsymbol{u}\right)\right] = -\nabla p + \nabla\cdot\left[\tilde{\mu}\left(\nabla\boldsymbol{u} + \nabla^T\boldsymbol{u}\right)\right] + \int_A \sigma_* \kappa \boldsymbol{n} \delta\left(\boldsymbol{x} - \boldsymbol{x}_\mathrm{f}\right) dA$$

# Newt. Two-Layer Airway Closure

Erken et al., JFM (2022)

## Mathematical Model

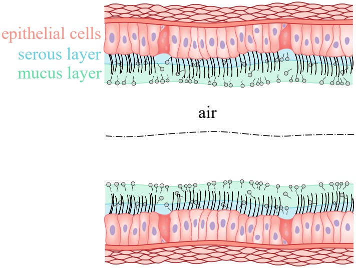


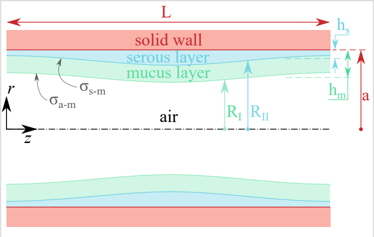


Newtonian two-layer airway closure model (clean)

$$\nabla \cdot \boldsymbol{u} = 0$$

$$\mathrm{La}\left[\frac{\partial\left(\tilde{\varrho}\boldsymbol{u}\right)}{\partial t} + \nabla\cdot\left(\tilde{\varrho}\boldsymbol{u}\boldsymbol{u}\right)\right] = -\nabla p + \nabla\cdot\left[\tilde{\mu}\left(\nabla\boldsymbol{u} + \nabla^T\boldsymbol{u}\right)\right] + \int_A \sigma_* \kappa \boldsymbol{n}\delta\left(\boldsymbol{x} - \boldsymbol{x}_\mathrm{f}\right) dA$$

Single-field approach: $\tilde{\varrho}(\phi_1, \phi_2)$, $\tilde{\mu}(\phi_1, \phi_2)$

Non-dimensional groups: $\mathrm{La} = \dfrac{\sigma_{\text{a-m}}\rho_\mathrm{m} a}{\mu_\mathrm{m}^2}$, $\varrho^* = \dfrac{\rho_\mathrm{a}}{\rho_\mathrm{m}}$, $\mu^* = \dfrac{\mu_\mathrm{a}}{\mu_\mathrm{m}}$, $\lambda = \dfrac{L}{a}$, $\sigma = \dfrac{\sigma_{\text{a-m}}}{\sigma_{\text{m-s}}}$

$$\varepsilon_\mathrm{m} = \frac{h_\mathrm{m} - h_\mathrm{s}}{a},\ \varepsilon_\mathrm{s} = \frac{h_\mathrm{s}}{a},\ \varepsilon = \frac{h_\mathrm{m}}{h_\mathrm{s}},\ \mu = \frac{\mu_\mathrm{m}}{\mu_\mathrm{s}},\ \rho = \frac{\rho_\mathrm{m}}{\rho_\mathrm{s}}$$

# Newt. Two-Layer Airway Closure

Erken et al., JFM (2022)

## Effect of Serous Layer

La $= 174$, $\lambda = 6$, $\mu = 10$, $\rho = 1$, $\sigma = 10$, $(\epsilon_{\mathrm{m}} + \epsilon_{\mathrm{s}}) = 0.2$, $\epsilon = 3$

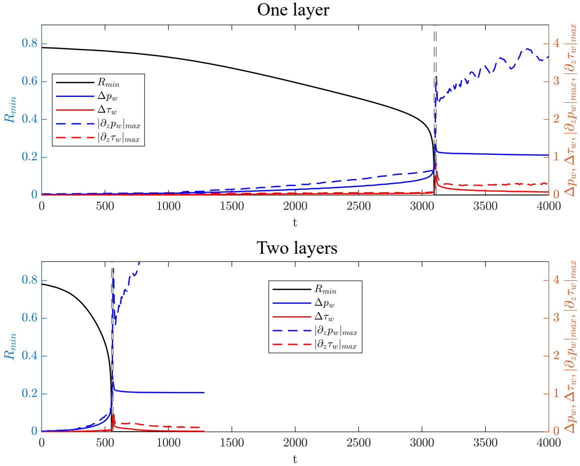

# Newt. Two-Layer Airway Closure

Erken et al., JFM (2022)

## Effect of Serous Layer

$\mathrm{La} = 174,\ \lambda = 6,\ \mu = 10,\ \rho = 1,\ \sigma = 10,\ (\epsilon_\mathrm{m} + \epsilon_\mathrm{s}) = 0.2,\ \epsilon = 3$

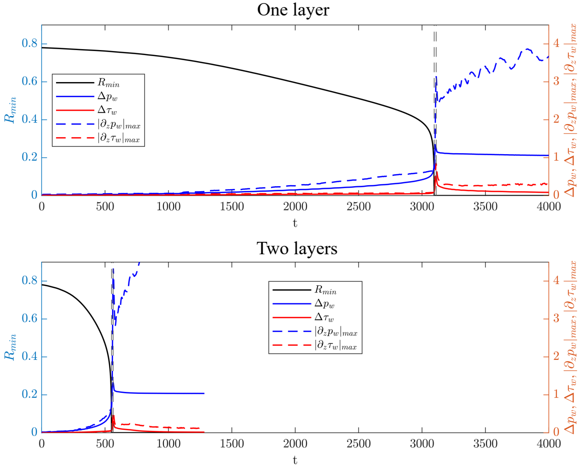


including a liquid layer speeds up the airway closure ($\times 6$)

# Newt. Two-Layer Airway Closure

Erken et al., JFM (2022)

## Effect of Mucus Layer Thickness

$\mathrm{La} = 174,\ \lambda = 6,\ \mu = 10,\ \rho = 1,\ \sigma = 10,\ \epsilon_\mathrm{s} = 0.05$

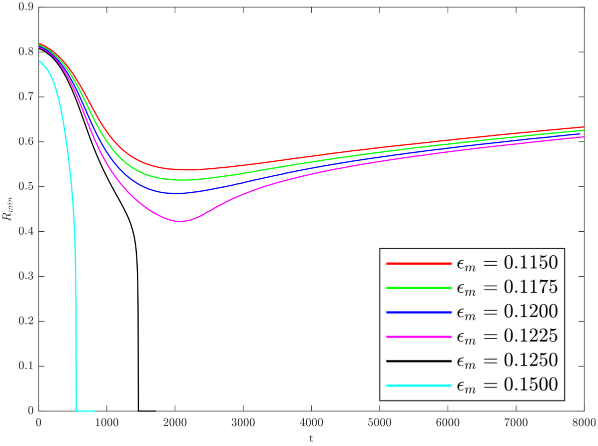

# Newt. Two-Layer Airway Closure

Erken et al., JFM (2022)

## Effect of Mucus Layer Thickness

La $= 174$, $\lambda = 6$, $\mu = 10$, $\rho = 1$, $\sigma = 10$, $\epsilon_s = 0.05$

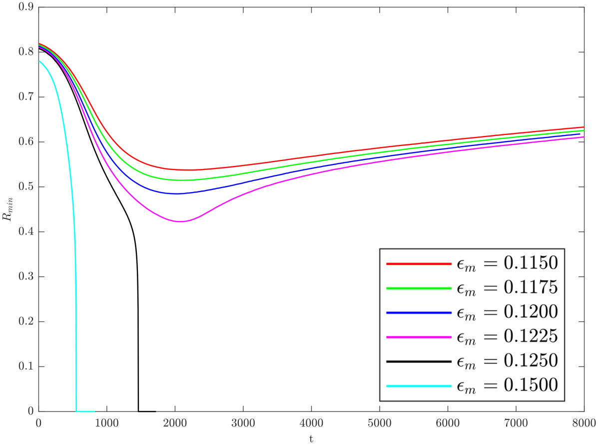


$\boxed{\epsilon_m \downarrow \text{ stabilizes the Plateau–Rayleigh instability for } \epsilon_m = 0.1225}$

# Newt. Two-Layer Airway Closure

Erken et al., JFM (2022)

## Effect of Serous Layer Thickness

$\mathrm{La} = 174,\ \lambda = 6,\ \mu = 10,\ \rho = 1,\ \sigma = 10,\ \epsilon_{\mathrm{m}} = 0.15$

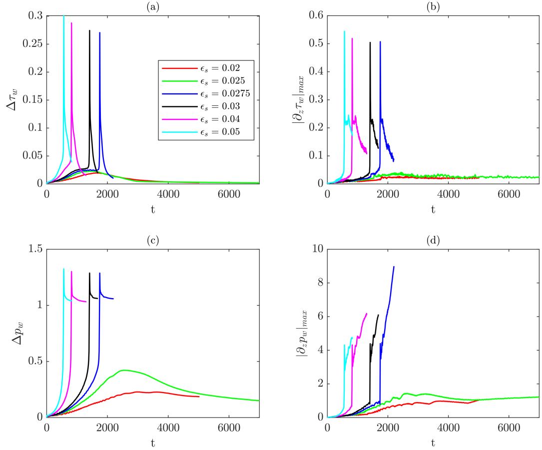

# Newt. Two-Layer Airway Closure

Erken et al., JFM (2022)

## Effect of Serous Layer Thickness

$\mathrm{La} = 174,\ \lambda = 6,\ \mu = 10,\ \rho = 1,\ \sigma = 10,\ \epsilon_\mathrm{m} = 0.15$

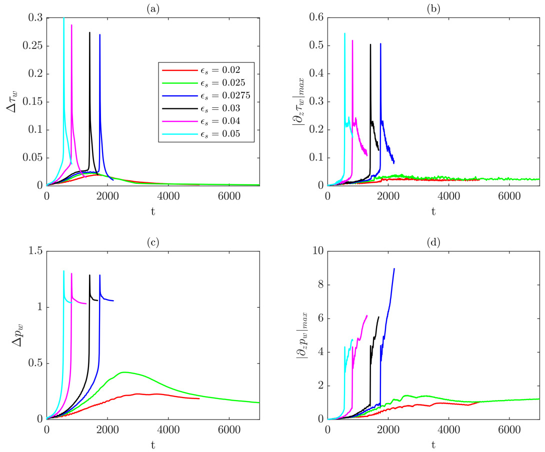


$\boxed{\epsilon_\mathrm{s} \downarrow \text{ stabilizes the Plateau–Rayleigh instability for } \epsilon_\mathrm{s} = 0.025}$

# Newt. Two-Layer Airway Closure

Erken et al., JFM (2022)

## Effect of Viscosity Ratio

$\mathrm{La} = 174,\ \lambda = 6,\ \rho = 1,\ \sigma = 10,\ (\epsilon_\mathrm{m} + \epsilon_\mathrm{s}) = 0.2,\ \epsilon = 3$

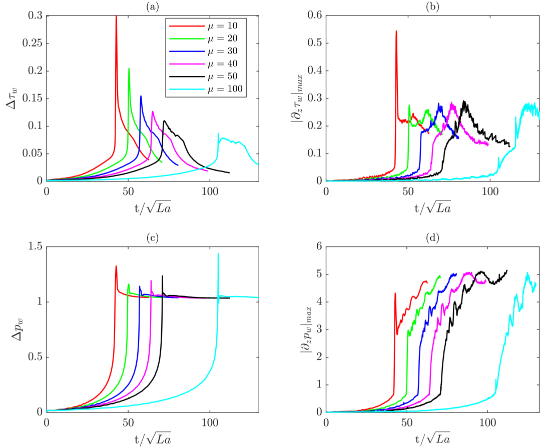

# Newt. Two-Layer Airway Closure

Erken et al., JFM (2022)

## Effect of Viscosity Ratio

La = 174, $\lambda = 6$, $\rho = 1$, $\sigma = 10$, $(\epsilon_m + \epsilon_s) = 0.2$, $\epsilon = 3$

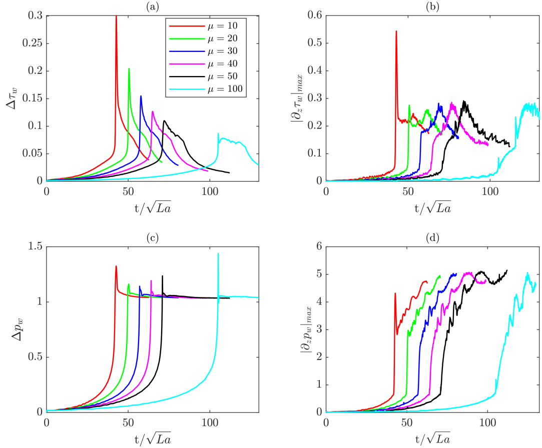


$\mu \uparrow$ reduces the shear stresses and does not impact the normal stresses

# Newt. Airway Closure + Surf.

Romanò et al., submit.

## Mathematical Model

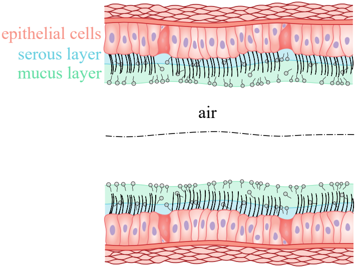


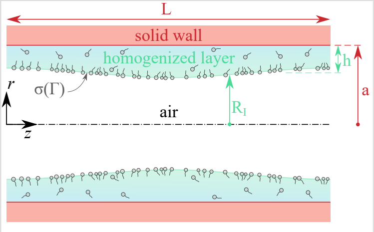

Newtonian airway closure model (contaminated)

$$\nabla \cdot \boldsymbol{u} = 0$$

$$\mathrm{La}\left[\frac{\partial\left(\tilde{\varrho}\boldsymbol{u}\right)}{\partial t} + \nabla\cdot\left(\tilde{\varrho}\boldsymbol{u}\boldsymbol{u}\right)\right] = -\nabla p + \nabla\cdot\left[\tilde{\mu}\left(\nabla\boldsymbol{u} + \nabla^T\boldsymbol{u}\right)\right] + \int_A \sigma(\Gamma)\kappa\boldsymbol{n}\delta\left(\boldsymbol{x}-\boldsymbol{x}_{\mathrm{f}}\right)dA + \int_A \nabla_s\sigma(\Gamma)\delta\left(\boldsymbol{x}-\boldsymbol{x}_{\mathrm{f}}\right)dA$$

Single-field approach: $\tilde{\varrho} = \phi + \varrho(1-\phi), \quad \tilde{\mu} = \phi + \mu(1-\phi)$

# Newt. Airway Closure + Surf.

Romanò et al., submit.

## Mathematical Model

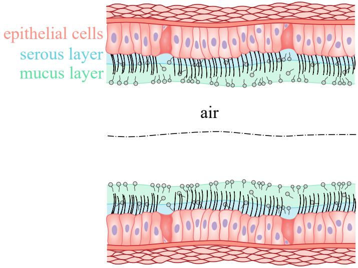


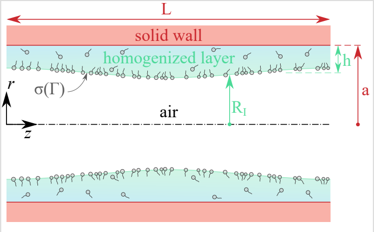


Newtonian airway closure model (contaminated)

$$\sigma = \begin{cases} (1-\beta\Gamma) & \text{if } \Gamma < 1, \\ (1-\beta)\exp\left[\dfrac{\beta(1-\Gamma)}{1-\beta}\right] & \text{if } \Gamma \geq 1. \end{cases} \qquad \text{where} \quad \beta = \frac{\mathcal{R}T\Gamma_\infty}{\sigma_0}$$

# Newt. Airway Closure + Surf.

Romanò et al., submit.

## Mathematical Model

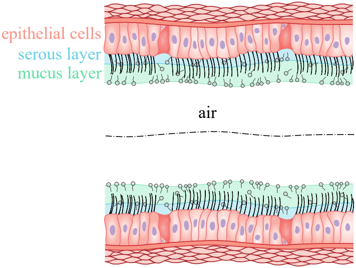


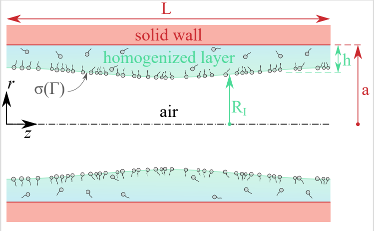


Newtonian airway closure model (contaminated)

$$\frac{1}{A}\frac{\mathrm{D}(\Gamma A)}{\mathrm{D}t} = \frac{1}{\mathrm{Sc_s La}}\nabla_s^2\Gamma + \dot{S}_\Gamma,$$

$$\frac{\partial C}{\partial t} + \nabla\cdot(C\boldsymbol{u}) = \frac{1}{\mathrm{ScLa}}\nabla\cdot\left(\tilde{D}\nabla C\right) + \dot{S}_C,$$

$$\dot{S}_\Gamma = \begin{cases} \dfrac{\mathrm{K_a}}{\mathrm{LaSc_s}}C_\mathrm{s}(1-\Gamma) - \dfrac{\mathrm{K_d}}{\mathrm{LaSc_s}}\Gamma & \text{if } \Gamma < 1, \\ -\dfrac{\mathrm{K_d}}{\mathrm{LaSc_s}}\Gamma & \text{if } \Gamma \geq 1, \end{cases}$$

# Newt. Airway Closure + Surf.

Romanò et al., submit.

## Mathematical Model

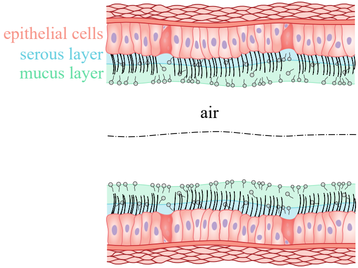


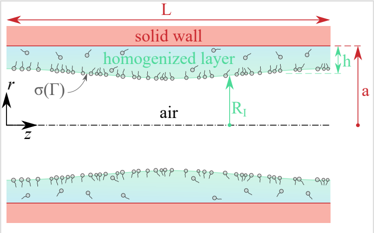

Newtonian airway closure model (contaminated)

Non-dimensional groups: $\mathrm{La} = \dfrac{\sigma_0 \rho_\mathrm{L} a}{\mu_\mathrm{L}^2}$, $\varrho = \dfrac{\rho_\mathrm{G}}{\rho_\mathrm{L}}$, $\mu = \dfrac{\mu_\mathrm{G}}{\mu_\mathrm{L}}$, $\lambda = \dfrac{L}{a}$, $\varepsilon = \dfrac{h}{a}$,

$$\beta = \frac{\mathcal{R} T \Gamma_\infty}{\sigma_0}, \ \mathrm{Sc} = \frac{\mu_\mathrm{L}}{\rho_\mathrm{L} D_\mathrm{L}}, \ \mathrm{Sc}_\mathrm{s} = \frac{\mu_\mathrm{L}}{\rho_\mathrm{L} D_\mathrm{S}},$$

$$\mathrm{K}_\mathrm{a} = \frac{k_\mathrm{a} C_\mathrm{cmc} a^2}{D_\mathrm{S}}, \ \mathrm{K}_\mathrm{d} = \frac{k_\mathrm{a} a^2}{D_\mathrm{S}}, \ \chi = \frac{\Gamma_\infty}{C_\mathrm{cmc} a},$$

Initial perturbation: $r = R_\mathrm{I}(t=0) = a - h[1 - 0.1 \times \cos(2\pi z/L)]$

# Newt. Airway Closure + Surf.

Romanò et al., PRF (2022)

## Dynamics of the Surfactant

$\mathrm{La} = 100$, $\beta = 0.7$, $\mathrm{Sc} = 10$, $\mathrm{Sc_s} = 100$, $\mathrm{K_a} = 10^4$, $\mathrm{K_d} = 10^2$, $\chi = 0.01$, $C_0 = 10^{-4}$, $\varepsilon = 0.25$

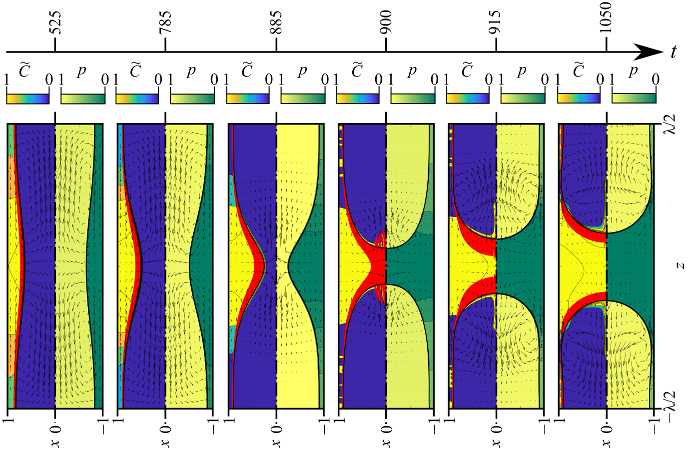

# Newt. Airway Closure + Surf.

Romanò et al., PRF (2022)

## Effect of Surfactant Concentration

$\mathrm{La} = 100,\ \beta = 0.7,\ \mathrm{Sc} = 10,\ \mathrm{Sc_s} = 100,\ \mathrm{K_a} = 10^4,\ \mathrm{K_d} = 10^2,\ \chi = 0.01,\ \varepsilon = 0.25$

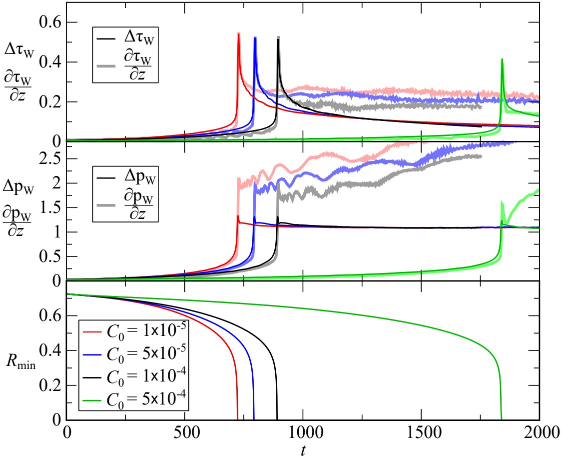

# Newt. Airway Closure + Surf.

Romanò et al., PRF (2022)

## Effect of Surfactant Concentration

$\mathrm{La} = 100,\ \beta = 0.7,\ \mathrm{Sc} = 10,\ \mathrm{Sc_s} = 100,\ \mathrm{K_a} = 10^4,\ \mathrm{K_d} = 10^2,\ \chi = 0.01,\ \varepsilon = 0.25$

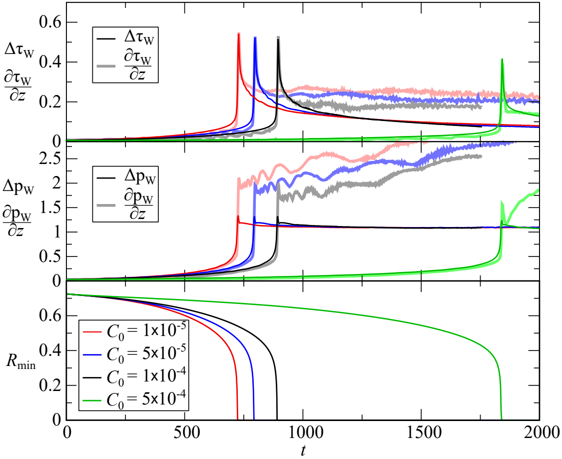


increasing $C_0$ slows down the closure and reduces the stresses

# Newt. Airway Closure + Surf. Romanò et al., PRF (2022)

## Effect of Surfactant Elasticity Parameter

$\mathrm{La} = 100$, $\chi = 0.01$, $\mathrm{Sc} = 10$, $\mathrm{Sc_s} = 100$, $\mathrm{K_a} = 10^4$, $\mathrm{K_d} = 10^2$, $C_0 = 10^{-4}$, $\varepsilon = 0.25$

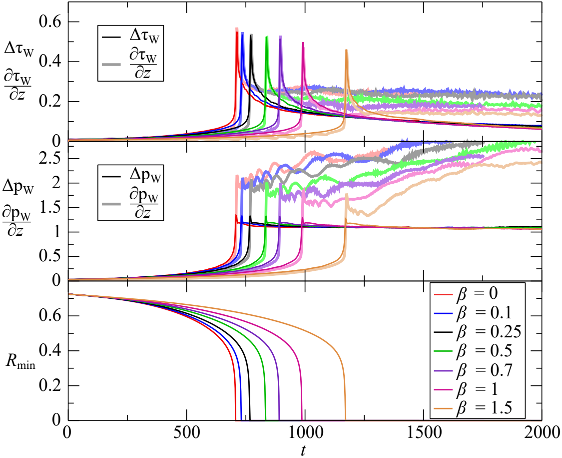

# Newt. Airway Closure + Surf.

Romanò et al., PRF (2022)

## Effect of Surfactant Elasticity Parameter

$\mathrm{La} = 100$, $\chi = 0.01$, $\mathrm{Sc} = 10$, $\mathrm{Sc_s} = 100$, $\mathrm{K_a} = 10^4$, $\mathrm{K_d} = 10^2$, $C_0 = 10^{-4}$, $\varepsilon = 0.25$

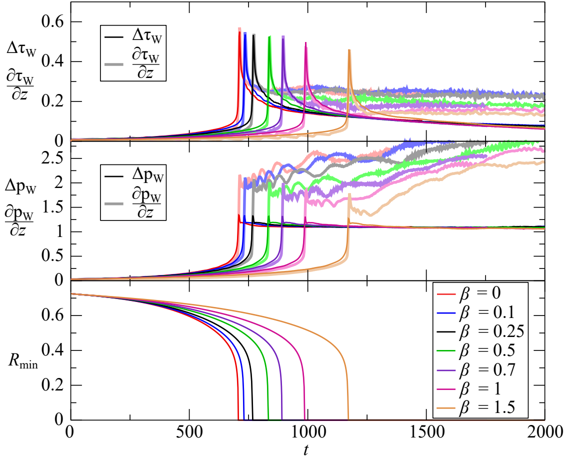


$\beta \uparrow$ slows down the closure and reduces the stresses

# Newt. Airway Closure + Surf. Romanò et al., PRF (2022)

## Effect of Penetration Depth

$\mathrm{La} = 100$, $\beta = 0.7$, $\mathrm{Sc} = 10$, $\mathrm{Sc_s} = 100$, $\mathrm{K_a} = 10^4$, $\mathrm{K_d} = 10^2$, $C_0 = 10^{-4}$, $\varepsilon = 0.25$

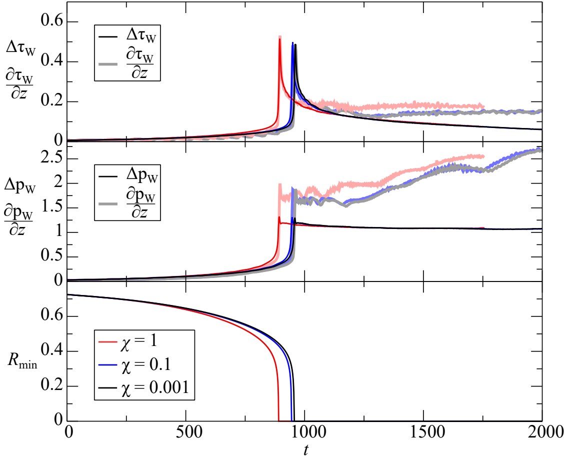

# Newt. Airway Closure + Surf.

Romanò et al., PRF (2022)

## Effect of Penetration Depth

$\mathrm{La} = 100,\ \beta = 0.7,\ \mathrm{Sc} = 10,\ \mathrm{Sc_s} = 100,\ \mathrm{K_a} = 10^4,\ \mathrm{K_d} = 10^2,\ C_0 = 10^{-4},\ \varepsilon = 0.25$

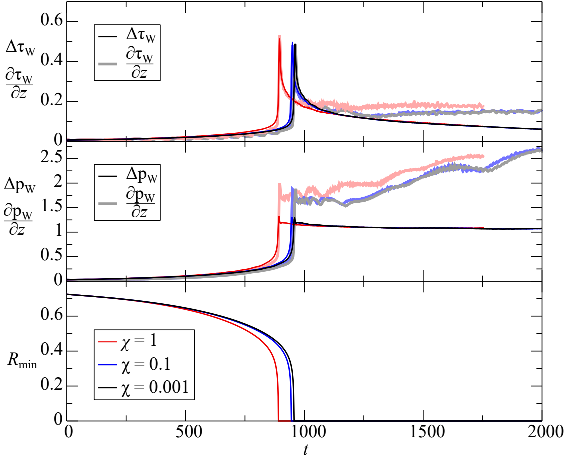


$\chi$ has little impact on the airway closure

# Newt. Airway Closure + Surf. Romanò et al., PRF (2022)

## Effect of Schmidt Numbers

$\mathrm{La} = 100$, $\chi = 0.01$, $\beta = 0.7$, $\mathrm{K_a} = 10^4$, $\mathrm{K_d} = 10^2$, $C_0 = 10^{-4}$, $\varepsilon = 0.25$

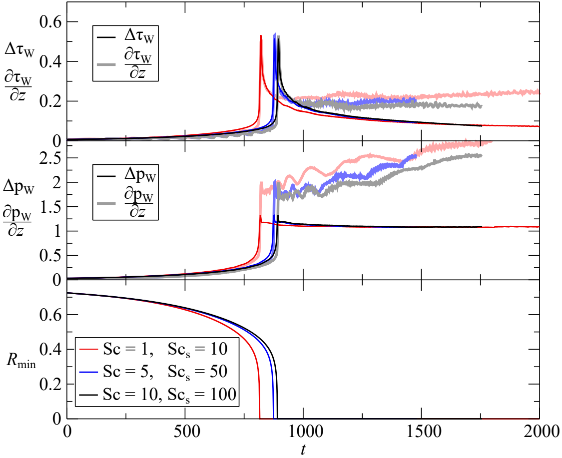

# Newt. Airway Closure + Surf.

Romanò et al., PRF (2022)

## Effect of Schmidt Numbers

$\mathrm{La} = 100$, $\chi = 0.01$, $\beta = 0.7$, $\mathrm{K_a} = 10^4$, $\mathrm{K_d} = 10^2$, $C_0 = 10^{-4}$, $\varepsilon = 0.25$

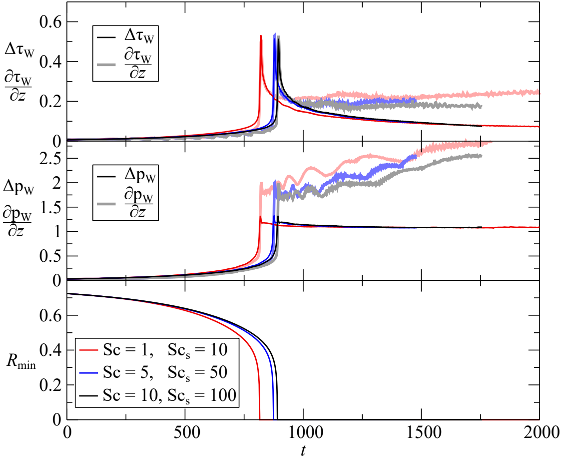


Sc and Sc$_s$ have little impact on the airway closure

# Newt. Airway Closure + Surf. Romanò et al., PRF (2022)

## Effect of Adsorption and Desorption Coefficients

$\mathrm{La} = 100$, $\chi = 0.01$, $\beta = 0.7$, $\mathrm{Sc} = 10$, $\mathrm{Sc_s} = 100$, $C_0 = 10^{-4}$, $\varepsilon = 0.25$

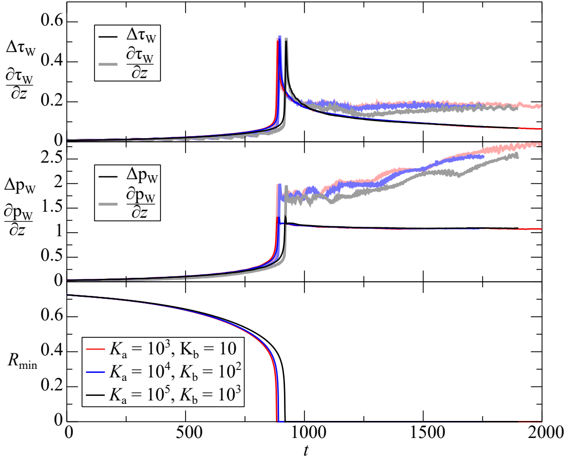

# Newt. Airway Closure + Surf.

Romanò et al., PRF (2022)

## Effect of Adsorption and Desorption Coefficients

$\mathrm{La} = 100$, $\chi = 0.01$, $\beta = 0.7$, $\mathrm{Sc} = 10$, $\mathrm{Sc_s} = 100$, $C_0 = 10^{-4}$, $\varepsilon = 0.25$

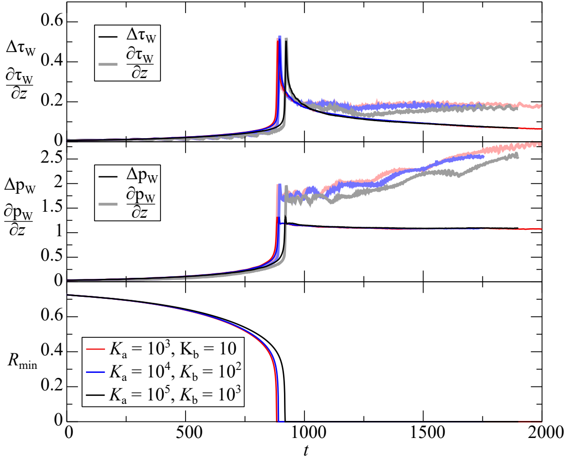


$\mathrm{K_a}$ and $\mathrm{K_d}$ have little impact on the airway closure

# Newt. Airway Closure + Surf.

Romanò et al., PRF (2022)

## Stability Analysis

La = 100, $\chi = 0.01$, $\beta = 0.7$, Sc = 10, $\mathrm{Sc_s} = 100$, $\mathrm{K_a} = 10^4$, $\mathrm{K_d} = 10^2$

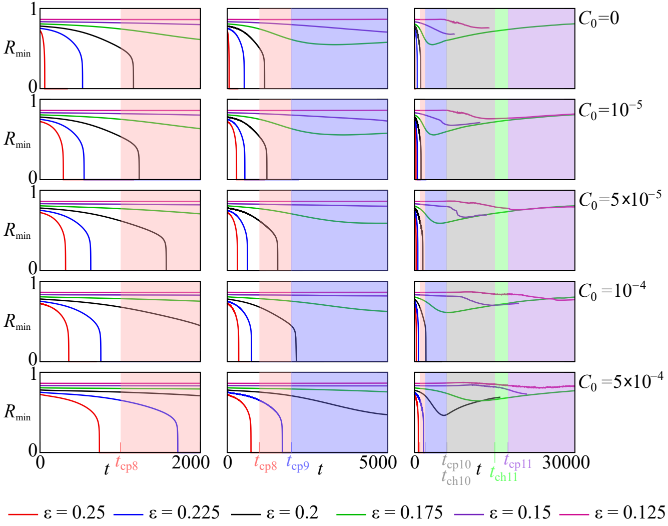

# Newt. Airway Closure + Surf.

Romanò et al., PRF (2022)

## Stability Analysis

$\mathrm{La} = 100$, $\chi = 0.01$, $\beta = 0.7$, $\mathrm{Sc} = 10$, $\mathrm{Sc_s} = 100$, $\mathrm{K_a} = 10^4$, $\mathrm{K_d} = 10^2$

● = physiologically stable ○ = physiologically unstable

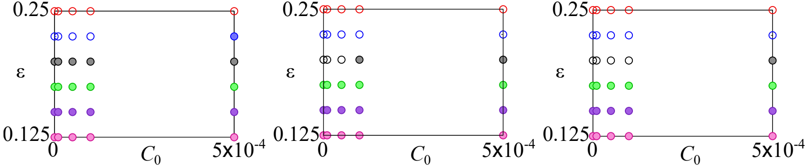


8-th gen. fast-breathing

9-th gen. fast-breathing

10-th gen. and higher

# Newt. Airway Closure + Surf.

Romanò et al., PRF (2022)

## Stability Analysis

La $= 100$, $\chi = 0.01$, $\beta = 0.7$, Sc $= 10$, $\mathrm{Sc_s} = 100$, $\mathrm{K_a} = 10^4$, $\mathrm{K_d} = 10^2$

$\bullet$ = physiologically stable $\circ$ = physiologically unstable

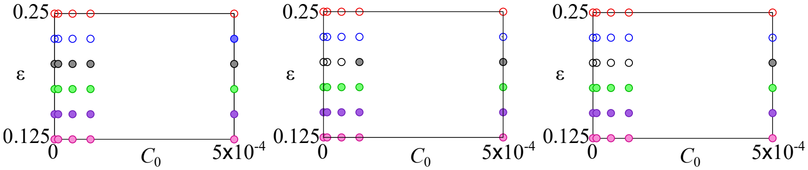


8-th gen. fast-breathing

9-th gen. fast-breathing

10-th gen. and higher

surfactant replacement can stabilize and shift closure to higher generations

# Viscoelastic Airway Closure

Romanò et al., JFM (2021)

## Mathematical Model

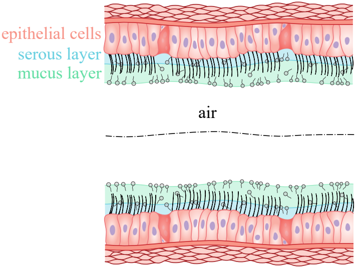


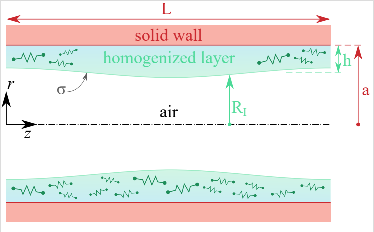


viscoelastic airway closure model (clean)

$$\nabla \cdot \boldsymbol{u} = 0$$

$$\mathrm{La}\left[\frac{\partial\left(\tilde{\varrho}\boldsymbol{u}\right)}{\partial t} + \nabla\cdot\left(\tilde{\varrho}\boldsymbol{u}\boldsymbol{u}\right)\right] = -\nabla p + \nabla\cdot\tilde{\boldsymbol{\tau}} + \int_A \sigma\kappa\boldsymbol{n}\delta\left(\boldsymbol{x}-\boldsymbol{x}_\mathrm{f}\right)dA$$

# Viscoelastic Airway Closure

Romanò et al., JFM (2021)

## Mathematical Model

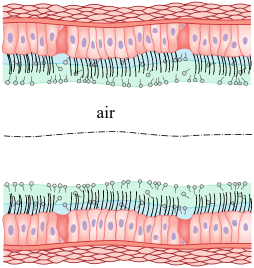


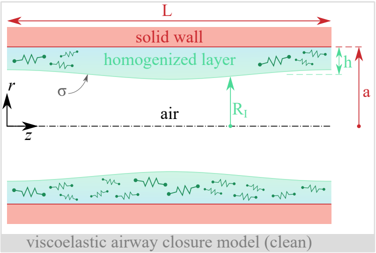


$$\nabla \cdot \boldsymbol{u} = 0$$

$$\mathrm{La}\left[\frac{\partial\left(\tilde{\varrho}\boldsymbol{u}\right)}{\partial t} + \nabla\cdot\left(\tilde{\varrho}\boldsymbol{u}\boldsymbol{u}\right)\right] = -\nabla p + \nabla\cdot\tilde{\boldsymbol{\tau}} + \int_A \sigma\kappa\boldsymbol{n}\delta\left(\boldsymbol{x}-\boldsymbol{x}_{\mathrm{f}}\right)dA$$

Single-field approach: $\tilde{\varrho} = \phi + \varrho(1-\phi)$, $\tilde{\boldsymbol{\tau}} = \left[\mu_{\mathrm{S}}\phi + \mu(1-\phi)\right]\left(\nabla\boldsymbol{u} + \nabla^T\boldsymbol{u}\right) + \phi\boldsymbol{S}$

Oldroyd-B: $\mathrm{We}\left[\partial_t\boldsymbol{S} + (\boldsymbol{u}\cdot\nabla)\,\boldsymbol{S} - (\nabla\boldsymbol{u})\,\boldsymbol{S} - \boldsymbol{S}\left(\nabla^{\mathrm{T}}\boldsymbol{u}\right)\right] + \boldsymbol{S} = \mu_{\mathrm{P}}\left(\nabla\boldsymbol{u} + \nabla^T\boldsymbol{u}\right)$

# Viscoelastic Airway Closure

Romanò et al., JFM (2021)

## Mathematical Model

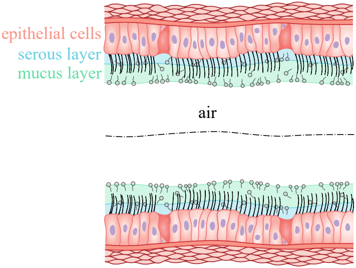


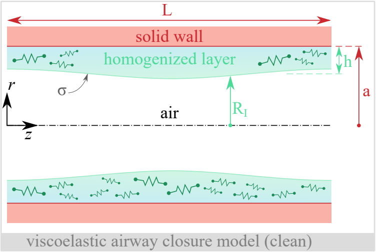


Non-dimensional groups: $\mathrm{La} = \dfrac{\sigma \rho_L a}{\mu_L^2}$, $\varrho = \dfrac{\rho_G}{\rho_L}$, $\mu = \dfrac{\mu_G}{\mu_L}$, $\lambda = \dfrac{L}{a}$, $\varepsilon = \dfrac{h}{a}$

$\mathrm{We} = \dfrac{\Lambda \sigma}{a \mu_L}$, $\mu_S = \dfrac{\mu_{L,S}}{\mu_L}$, $\mu_P = 1 - \mu_S$, ($\mathcal{L}^2$for FENE-CR)

Initial perturbation: $r = R_I(t=0) = a - h[1 - 0.1 \times \cos(2\pi z/L)]$

# Viscoelastic Airway Closure

Romanò et al., JFM (2021)

## Effect of Viscoelasticity (Oldroyd-B)

$\mu = 1.5 \times 10^{-4}$, $\varrho = 10^{-3}$, $\epsilon = 0.25$, $\lambda = 6$, $\mu_{\mathrm{S}} = 0.5$, $\mathrm{We} = 100$

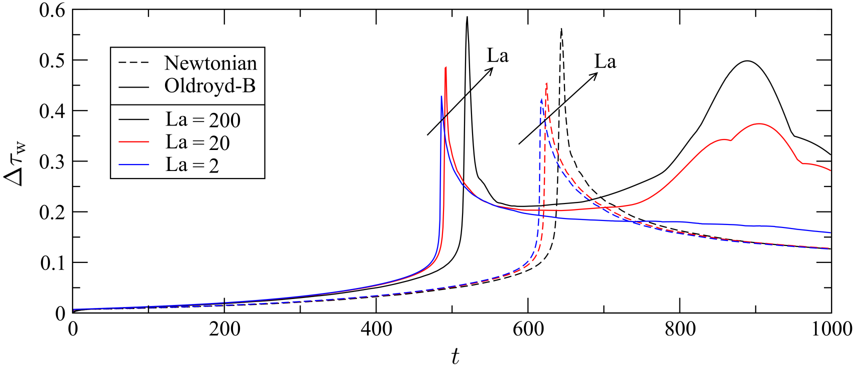

# Viscoelastic Airway Closure

Romanò et al., JFM (2021)

## Effect of Viscoelasticity (Oldroyd-B)

$\mu = 1.5 \times 10^{-4}$, $\varrho = 10^{-3}$, $\epsilon = 0.25$, $\lambda = 6$, $\mu_S = 0.5$, $\mathrm{We} = 100$

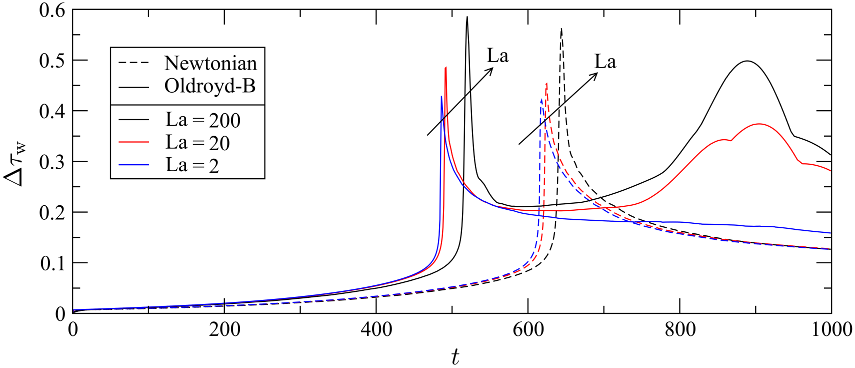


qualitative difference between Newtonian and viscoelastic

# Viscoelastic Airway Closure

Romanò et al., JFM (2021)

## Effect of Viscoelasticity (FENE-CR)

$\mu = 1.5 \times 10^{-4}$, $\varrho = 10^{-3}$, $\epsilon = 0.25$, $\lambda = 6$, $\mu_S = 0.5$, We $= 100$

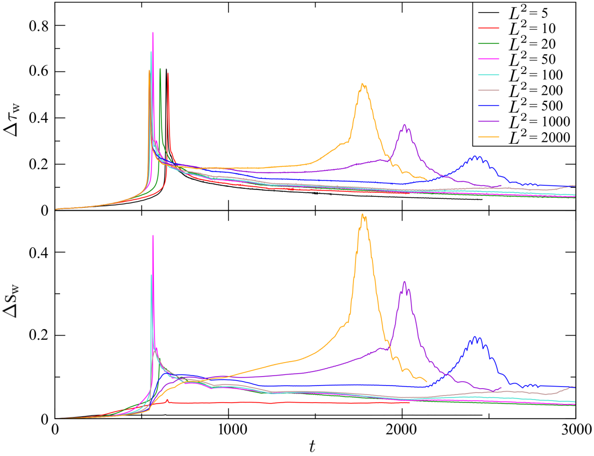

# Viscoelastic Airway Closure

Romanò et al., JFM (2021)

## Effect of Viscoelasticity (FENE-CR)

$\mu = 1.5 \times 10^{-4}$, $\varrho = 10^{-3}$, $\epsilon = 0.25$, $\lambda = 6$, $\mu_S = 0.5$, $We = 100$

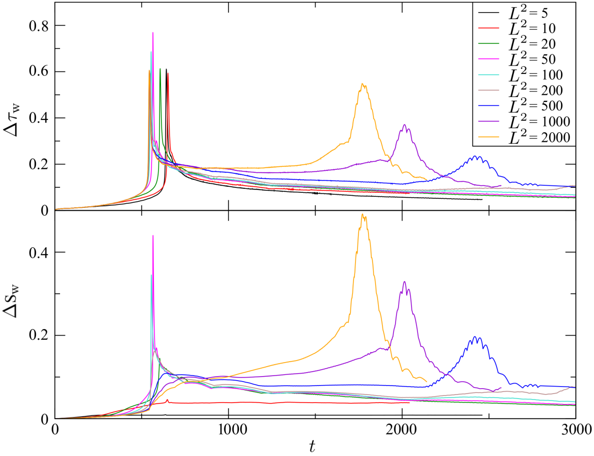


second hump robust to viscoelastic model

# Viscoelastic Airway Closure

Romanò et al., JFM (2021)

## Viscoelastic Instability Mechanism

La $= 2$, $\mu = 1.5 \times 10^{-4}$, $\varrho = 10^{-3}$, $\epsilon = 0.25$, $\lambda = 6$, $\mu_{\mathrm{S}} = 0.25$, We $= 500$

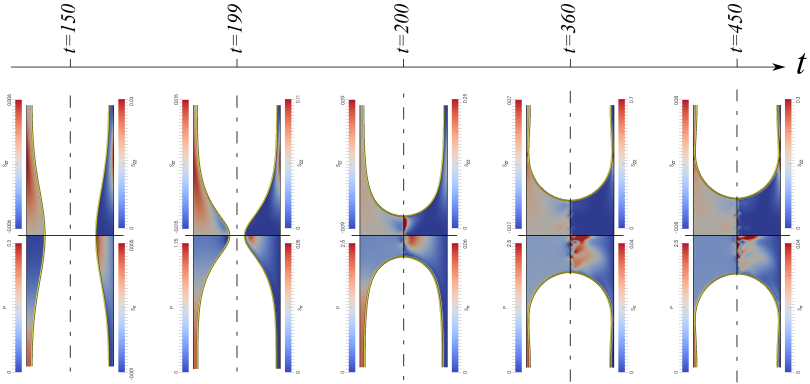

# Viscoelastic Airway Closure

Romanò et al., JFM (2021)

## Viscoelastic Instability Mechanism

$\mathrm{La} = 2$, $\mu = 1.5 \times 10^{-4}$, $\varrho = 10^{-3}$, $\epsilon = 0.25$, $\lambda = 6$, $\mu_{\mathrm{S}} = 0.25$, $\mathrm{We} = 500$

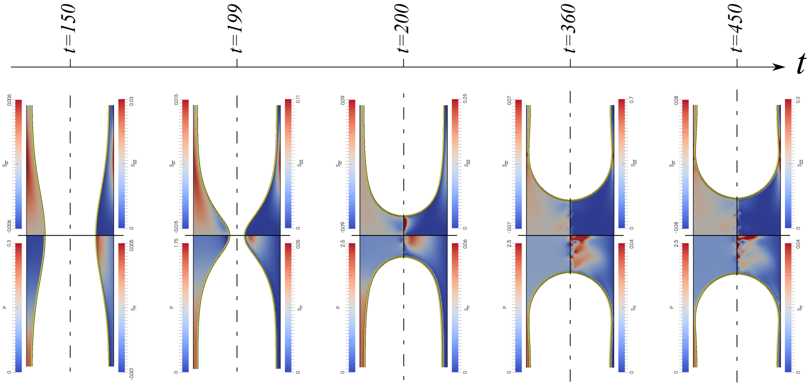


instability due to curvature of the streamlines

# Viscoelastic Airway Closure

Romanò et al., JFM (2021)

## Effect of Flow and Polymeric Parameters

$\mu = 1.5 \times 10^{-4}$, $\varrho = 10^{-3}$, $\epsilon = 0.25$, $\lambda = 6$,

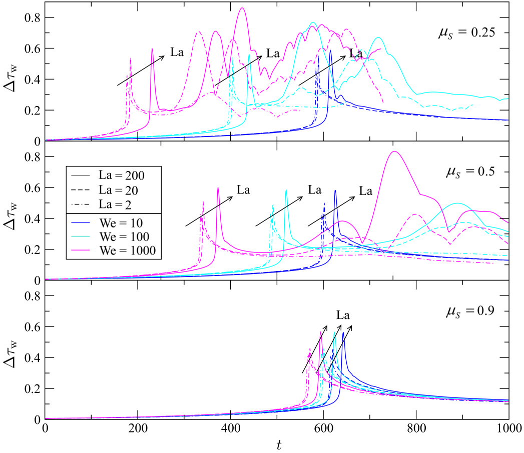


# Viscoelastic Airway Closure

Romanò et al., JFM (2021)

## Effect of Flow and Polymeric Parameters

$\mu = 1.5 \times 10^{-4}$, $\varrho = 10^{-3}$, $\epsilon = 0.25$, $\lambda = 6$,

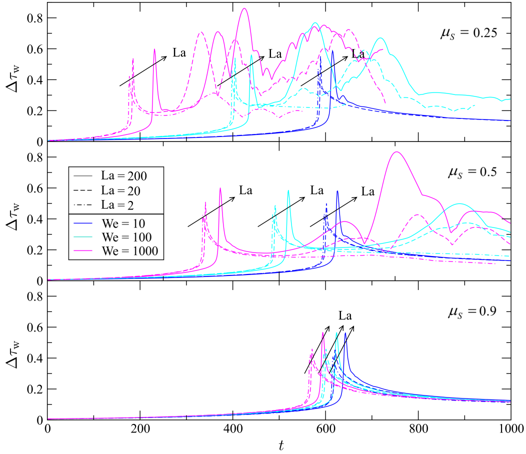


the instability depends on La, We, and $\mu_S$

# Viscoelastic Airway Closure

Romanò et al., JFM (2021)

## Elasto-Inertial Instability

$\mu = 1.5 \times 10^{-4}$, $\varrho = 10^{-3}$, $\epsilon = 0.25$, $\lambda = 6$,

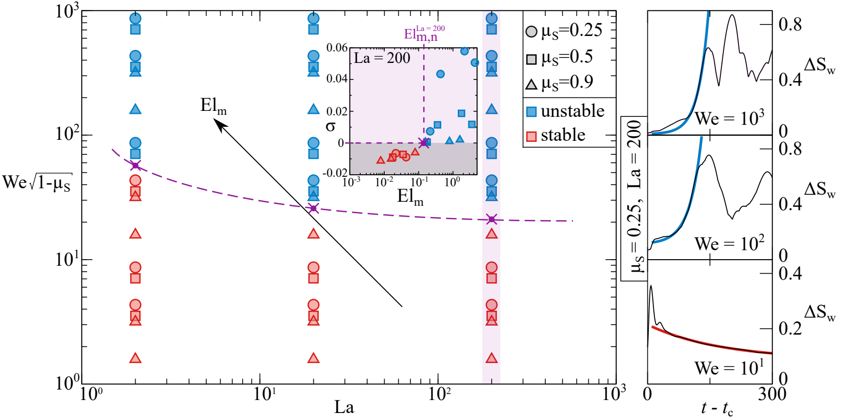

# Viscoelastic Airway Closure

Romanò et al., JFM (2021)

## Elasto-Inertial Instability

$\mu = 1.5 \times 10^{-4}$, $\varrho = 10^{-3}$, $\epsilon = 0.25$, $\lambda = 6$,

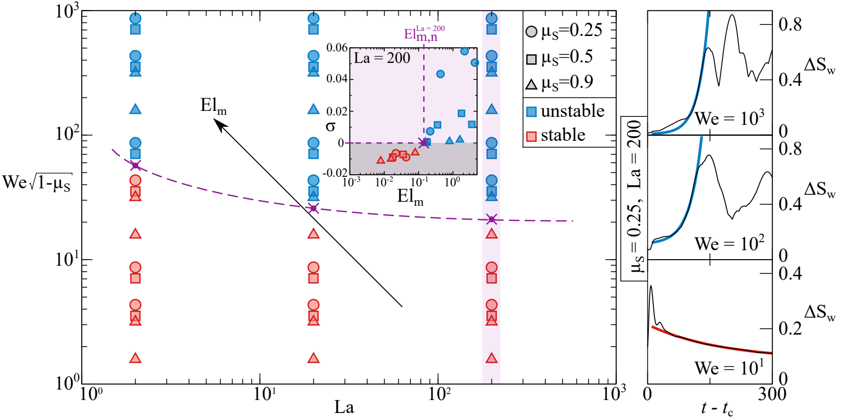


elasto-inertial instability

# Conclusions

Support from NIH (R01-HL136141) and from TUKITAK (119M513)

# Conclusions

- Numerical simulations well reproduce the experiments

Support from NIH (R01-HL136141) and from TUKITAK (119M513)

# Conclusions

- Numerical simulations well reproduce the experiments
- Liquid film coalescence induces high stress levels

Support from NIH (R01-HL136141) and from TUKITAK (119M513)

# Conclusions

- Numerical simulations well reproduce the experiments
- Liquid film coalescence induces high stress levels
- Quick bi-frontal plug growth: post-coalescence stress mechanism

Support from NIH (R01-HL136141) and from TUKITAK (119M513)

## Conclusions

- Numerical simulations well reproduce the experiments
- Liquid film coalescence induces high stress levels
- Quick bi-frontal plug growth: post-coalescence stress mechanism
- Bi-frontal plug growth can injury the epithelial cells

Support from NIH (R01-HL136141) and from TUKITAK (119M513)

# Conclusions

- Numerical simulations well reproduce the experiments
- Liquid film coalescence induces high stress levels
- Quick bi-frontal plug growth: post-coalescence stress mechanism
- Bi-frontal plug growth can injury the epithelial cells
- The two-layer airway closure is much faster than the single-layer one

Support from NIH (R01-HL136141) and from TUKITAK (119M513)

# Conclusions

- Numerical simulations well reproduce the experiments
- Liquid film coalescence induces high stress levels
- Quick bi-frontal plug growth: post-coalescence stress mechanism
- Bi-frontal plug growth can injury the epithelial cells
- The two-layer airway closure is much faster than the single-layer one
- The stability limits are strongly affected by the two-layer dynamics

Support from NIH (R01-HL136141) and from TUKITAK (119M513)

# Conclusions

- Numerical simulations well reproduce the experiments
- Liquid film coalescence induces high stress levels
- Quick bi-frontal plug growth: post-coalescence stress mechanism
- Bi-frontal plug growth can injury the epithelial cells
- The two-layer airway closure is much faster than the single-layer one
- The stability limits are strongly affected by the two-layer dynamics
- Increasing the mucus-to-serous viscosity ratio decreases the stresses

Support from NIH (R01-HL136141) and from TUKITAK (119M513)

# Conclusions

- Numerical simulations well reproduce the experiments
- Liquid film coalescence induces high stress levels
- Quick bi-frontal plug growth: post-coalescence stress mechanism
- Bi-frontal plug growth can injury the epithelial cells
- The two-layer airway closure is much faster than the single-layer one
- The stability limits are strongly affected by the two-layer dynamics
- Increasing the mucus-to-serous viscosity ratio decreases the stresses
- Double coalescence is observed for two-layer airway closure

Support from NIH (R01-HL136141) and from TUKITAK (119M513)

# Conclusions

- ▷ Numerical simulations well reproduce the experiments
- ▷ Liquid film coalescence induces high stress levels
- ▷ Quick bi-frontal plug growth: post-coalescence stress mechanism
- ▷ Bi-frontal plug growth can injury the epithelial cells
- ▷ The two-layer airway closure is much faster than the single-layer one
- ▷ The stability limits are strongly affected by the two-layer dynamics
- ▷ Increasing the mucus-to-serous viscosity ratio decreases the stresses
- ▷ Double coalescence is observed for two-layer airway closure
- ▷ At high We, elasto-inertial instability induces severe extra stresses

Support from NIH (R01-HL136141) and from TUKITAK (119M513)

# Conclusions

- ▷ Numerical simulations well reproduce the experiments
- ▷ Liquid film coalescence induces high stress levels
- ▷ Quick bi-frontal plug growth: post-coalescence stress mechanism
- ▷ Bi-frontal plug growth can injury the epithelial cells
- ▷ The two-layer airway closure is much faster than the single-layer one
- ▷ The stability limits are strongly affected by the two-layer dynamics
- ▷ Increasing the mucus-to-serous viscosity ratio decreases the stresses
- ▷ Double coalescence is observed for two-layer airway closure
- ▷ At high We, elasto-inertial instability induces severe extra stresses
- ▷ Surfactant reduces the wall stresses and postpones the airway closure

Support from NIH (R01-HL136141) and from TUKITAK (119M513)